RANK signaling blockade reduces breast cancer recurrence by inducing tumor cell differentiation

Guillermo Yoldi[1*], Pasquale Pellegrini[1*&], Eva M. Trinidad[1*], Alex Cordero[1], Jorge Gomez-Miragaya[1], Jordi Serra-Musach[2], William C Dougall[3&], Purificación Muñoz[1], Miguel-Angel Pujana[2], Lourdes Planelles[4] and Eva González-Suarez[1, #]

[1]Cancer Epigenetics and Biology Program, Bellvitge Biomedical Research Institute, IDIBELL, Barcelona, Spain.

[2]Program Against Cancer Therapeutic Resistance (ProCURE), Breast Cancer and Systems Biology Lab, Catalan Institute of Oncology, IDIBELL, Barcelona, Spain.

[3] Therapeutic Innovation Unit, Amgen Inc., Seattle, WA, USA

[4]Centro Nacional de Biotecnología/CSIC, UAM Cantoblanco, 28049 Madrid, Spain.

[*] contributed equally

[#]Corresponding author: Eva González-Suárez

Cancer Epigenetics and Biology Program, Bellvitge Institute for Biomedical Research, IDIBELL.

Av. Gran Via de L'Hospitalet, 199, 08908 L'Hospitalet de Llobregat, Barcelona, Spain

egsuarez@idibell.cat

Phone: +34 932607139 Fax: +34 932607219

www.pebc.cat

& current address:

PP: Gladstone Institutes, 1650 Owens Street, 94158 San Francisco, California, USA

WCD: Department of Immunology in Cancer and Infection, QIMR Berghofer Medical Research Institute, Herston, QLD, Australia

RUNNING TITLE: Therapeutic RANKL inhibition reduces cancer stem cells

KEYWORDS: RANK, breast cancer, cancer stem cells, tumor differentiation therapy

CONFLICT OF INTEREST: WC Dougall is employee and stockholder of Amgen Inc. All others declare they have no conflict of interest.

FINANCIAL SUPPORT

This work was supported by grants to E. González-Suárez by MINECO and ISCIII (SAF2011-22893, SAF2014-55997; PIE13/00022, co-funded by FEDER funds/European Regional Development Fund (ERDF)- a way to build Europe-) and by the Susan Komen Foundation CCR13262449, Concern Foundation, Fundació La Marató, to M.A. Pujana from ISCIII (PI12/01528) and AGAUR (SGR 2014-364), and to L. Planelles from ISCIII (PI10/01556). P Pellegrini and J Gomez-Miragaya are recipients of an FPI grant from MINECO. The funders had no role in study design, data collection and analysis, decision to publish, or preparation of the manuscript.

ABSTRACT

RANK expression is associated with poor prognosis in breast cancer even though its therapeutic potential remains unknown. RANKL and its receptor RANK are downstream effectors of the progesterone signaling pathway. However, RANK expression is enriched in hormone receptor negative adenocarcinomas suggesting additional roles for RANK signaling beyond its hormone-dependent function. Here, to explore the role of RANK signaling once tumors have developed we use the mouse mammary tumor virus- Polyoma Middle T (MMTV-PyMT) which mimics RANK and RANKL expression patterns seen in human breast adenocarcinomas. Complementary genetic and pharmacological approaches demonstrate that therapeutic inhibition of RANK signaling drastically reduces the cancer stem cell pool, decreases tumor and metastasis initiation and enhances sensitivity to chemotherapy. Mechanistically, genome wide expression analyses showed that anti-RANKL therapy promotes lactogenic differentiation of tumor cells. Moreover, RANK signaling in tumor cells negatively regulates the Ap2 transcription factors, and enhances the Wnt agonist *Rspo1* and the Sca1- population, enriched in tumor initiating cells. Additionally, we found that expression of *TFAP2B* and the RANK inhibitor, *OPG,* in human breast cancer correlate and are associated with relapse free tumors. These results support the use of RANKL inhibitors to reduce recurrence and metastasis in breast cancer patients based on its ability to induce tumor cell differentiation.

INTRODUCTION

Multiple lines of evidence support the existence of tumor initiating cells or cancer stem cells (CSCs) in breast cancer (1). Recent efforts to develop CSC-related therapies explored elimination of the CSC population, removal of self-renewal capability and forced terminal differentiation. The first differentiation agent successfully used in the clinic was all-trans retinoic acid in acute promyelocytic leukemia (2). Retinoid signaling also regulates breast CSC self renewal and differentiation (3).

Receptor activator of NF-kappaB ligand (RANKL) is expressed in progesterone receptor-positive (PR+) mammary epithelial cells and acts as a paracrine mediator of progesterone in mouse and human mammary epithelium (4-9). Overexpression of RANKL's receptor, RANK in mammary epithelial cells enhances proliferation, impairs lactation and induces the accumulation of mammary stem cells (MaSC) and progenitors (9-12). In human adenocarcinomas RANK is predominantly expressed in hormone receptor-negative (HR-) tumors, supporting a progesterone-independent role. In contrast to RANK, RANKL is rarely expressed on tumor cells, but it is expressed in tumor-infiltrating lymphocytes (7, 11, 13). RANK expression in human adenocarcinomas is associated with reduced overall survival (13, 14). However, the mechanisms underlying these aggressive tumor phenotypes and the therapeutic potential of RANKL inhibition once tumors have developed remain unexplored.

The MMTV-PyMT breast cancer mouse model displays widespread transformation of the mammary gland and a high incidence of lung metastasis (15, 16). Tumor cells of invasive PyMT adenocarcinomas do not express hormone receptors or RANKL, but do express high levels of RANK (7, 9). RANKL inhibitors are currently used for the treatment of bone related pathologies, osteoporosis and bone metastasis. Here we demonstrate that inhibition

of RANK signaling acts as a differentiation therapy in breast cancer, depleting the cancer stem cells population and reducing recurrence and metastasis.

MATERIALS AND METHODS

Animals, RANKL, RANK-Fc and docetaxel treatments

All research involving animals was performed at the IDIBELL animal facility in compliance with protocols approved by the IDIBELL Committee on Animal Care and following national and European Union regulations. MMTV-PyMT (FVB/N-Tg(MMTV-PyVT)634Mul) were obtained from the Jackson Laboratory (15). MMTV-PyMT$^{-/+}$;RANK$^{-/-}$ mice were obtained by backcrossing the MMTV-PyMT (FvB/N) strain with RANK$^{+/-}$ mice into the C57BL/6 background (17). RANKL (25 1 mg/Kg) and RANK-Fc (10 mg/kg, Amgen) were injected subcutaneously three times a week (7, 10). Docetaxel (Actavis, 20 mg/ml) was administered at 25 mg/kg intraperitoneally twice per week..

Tumor cell isolation, tumor and metastasis initiation assays

Tumor cells were isolated as described (18). For orthotopic transplants and tumor-limiting dilution assays tumor cells were mixed 1:1 with Matrigel matrix (BD Biosciences) and orthotopically implanted in the inguinal mammary gland of 6-10-week-old syngeneic females. For metastasis assays tumor cells resuspended in cold PBS were injected intravenously in 6-10-week-old *Foxn1*^{nu} females.

Tissue histology and immunostaining

Tissue samples were fixed in formalin and embedded in paraffin. 3-μm sections were cut for histological analysis and stained with hematoxylin and eosin. Entire lungs were step-sectioned at 100 μm and 15 cuts per lung were quantified. Antigen heat retrieval with citrate was used for PR (DAKO), SMA-1 (Sigma-Aldrich), mRANKL (R&D Systems), Ki67 (Thermo Scientific), cleaved caspase-3 (Cell Signaling) antibodies and rabbit anti-

milk serum (kindly provided by Prof. Nancy E. Hynes). mRANK (R&D Systems) immunostaining was performed, pre-treating sections with Protease XXIV 5 U/mL (Sigma-Aldrich) for 15 min at room temperature. All antibodies were incubated overnight at 4°C, detected with biotinylated secondary antibodies and streptavidin horseradish peroxidase (Vector) and revealed with DAB substrate (DAKO).

Tumorsphere culture

Cells isolated from primary tumors were resuspended in serum-free DMEM F12 mammosphere medium containing 20 ng/mL of EFG, 1x B27 and 4 μg/mL heparin (Sigma-Aldrich), as previously described (19) with 2% of growth factor reduced matrigel. Primary tumorspheres were derived by plating 20,000 cells/mL in 2 mL of medium onto cell-suspension culture plates. After 14 days, tumorspheres were isolated by 5 min treatment with PBS-EDTA 1 mM + 5 min of trypsin at 37°C and plated for secondary tumorsphere formation at a concentration of 5,000 cells/mL in triplicate. Individual spheres from each replicate well were counted under a microscope.

Flow cytometry

Single cells were resuspended and blocked with PBS 2% FBS and IgG blocking reagent for 10 min on ice and incubated for 30 min on ice with CD45-APC-Cy7 (30-F11), CD4-PE-Cy7 (RM4-5), CD11b-APC (M1/70), CD8-PE or CD8-FITC (53-6.7), Gr1-FITC (RB6-8C5), F4/80-PE (BM8), CD49b-Alexa 647 (1HMa2), CD45-PECy7 or –APCCy7 (30-F11) and CD31-PECy7 (390) from Biolegend, CD24-FITC (M1/69), CD61-FITC (2C9.G2), Sca-1-APC (Ly-6A/E) from BD Pharmingen, CD90-PE (HIS51, Bioscience) and CD49f-a647 (GoH3, R&D Systems). FACS analysis was performed using FACS Canto, FACS

Aria (Becton Dickinson) and Diva software. Cells were sorted using MoFlo (Beckman Coulter) at 25 psi and a 100-µm tip.

RNA labeling and hybridization to Agilent microarrays

Hybridization to SurePrint G3 Mouse Gene Expression Microarray (ID G4852A, Agilent Technologies) was conducted following manufacturer's protocol (Two-Color Microarray-Based Gene Expression Analysis v. 6.5, Agilent Technologies), and dye swaps (Cy3 and Cy5) were performed for RNA amplified from each sample. Microarray chips were washed and scanned using a DNA Microarray Scanner (Model G2505C, Agilent Technologies).

Microarray analysis

Microarray data were feature extracted using Feature Extraction Software (v. 10.7) available from Agilent, using the default variables. Outlier features on the arrays were flagged by the same software package. Data analysis was performed using *Bioconductor* package, under R environment. Data preprocessing and differential expression analysis was performed using *limma* and *RankProd* package, and latest gene annotations available was used. Raw feature intensities were background corrected using *normexp* background correction algorithm. Within-array normalization was done using spatial and intensity-dependent *loess. Aquantile* normalization was used to normalize between arrays. The expression of each gene is reported as the *base 2 logarithm* of ratio of the value obtained of each condition relative to controls. A gene is considered differentially expressed if it displays a *pfp* (proportion of *false positives)* less than 0.05 by non-parametric test. The GSEA was run using default values for all parameters. Raw microarray data has been

deposited in GEO, access number GSE66085. The mature luminal and stem cell gene sets were taken from the original publication (20). The differentially expressed genes between lactation and pregnancy were identified using the GEO GSE8191 dataset (21) and the TFAP2C regulated genes in breast cancer cells using the GEO GSE8640 dataset (22). Cox proportional hazard regression analyses were applied to evaluate associations with prognosis (relapse or distant metastasis) at the level of microarray probes

Statistical analysis

Differences were analyzed with a two-tailed Student's t-test or an F-test, one sample t test against a reference value of 1. Two-way analysis of variance was used to compare tumor growth curves. The Mantel-Cox test was used for tumor-free survival studies. Frequency of tumor-initiating was estimated using the extreme limiting dilution assay (ELDA) (23). The statistical significance of difference between groups was expressed by asterisks (*, $0.01 < P < 0.05$; **, $0.001 < P < 0.01$; ***, $0.001 < P < 0.0001$; ****, $P<0.0001$).

RESULTS

RANKL stimulation promotes tumor growth in MMTV-PyMT primary tumor cells

MMTV-PyMT preneoplasic lesions and adenocarcinomas expressed high levels of RANK (Fig. 1A, B). RANKL expression was found in non-tumorigenic ducts and hyperplasias (Fig. 1A) but was lost in MMTV-PyMT adenocarcinomas, consistent with the loss of PR positivity (Fig. 1A, S1) (24). RANKL was expressed in draining lymph nodes and tumor infiltrating leucocytes of tumor-bearing mice (Fig. 1A-B). *Rankl* mRNA was predominantly found in tumor-infiltrating CD4+ and CD8+ T lymphocytes (CD45+CD11b-CD4+ and CD45+CD11b-CD8+), whereas *Rank* mRNA was found in tumor cells and macrophages (Fig. 1C, S2), consistent with the expression of RANK and RANKL in human breast adenocarcinomas (7, 11, 13), highlighting the relevance of the MMTV-PyMT tumor model to the study of human pathology.

Administration of RANKL resulted in increased acinar size in MMTV-PyMT tumor acini (Fig. S3A-B) (25, 26). No significant changes in proliferation were found, but decreased apoptosis was observed in RANKL-treated tumor cultures (Fig. S3B). RANKL-treated acini showed an "invasive-like" phenotype, with isolated cells surrounding the acini (Fig. S3A). Remarkably, 2-week RANKL-treated acini gave rise to faster growing tumors and more metastasis than untreated controls when injected in immunodeficient mice (Fig. S3C-D). These results demonstrate that activation of RANK signaling could promote tumor growth and metastasis in MMTV-PyMT primary tumor cells.

Inhibition of RANKL signaling decreases the frequency of tumor-initiating cells

No significant changes in tumor growth, tumor cell proliferation or apoptosis were observed after 2 weeks of RANKL treatment in vivo on tumor bearing MMTV-PyMT mice

(Fig. 1D-E, S3E) (10), but higher cell density was observed in contrast to control mice where extensive areas of dilated ducts and hyperplasias full of milk secretions were observed (Fig. 1F-G). These results indicate that short-term *in vivo* activation of RANK signaling is not sufficient to change the growth of established tumors, but appears to prevent secretory differentiation of tumor cells.

The putative benefit of pharmacological RANKL inhibition with RANK-Fc in tumor recurrence was interrogated (Fig 2A) (7). No significant differences in tumor growth or the frequency of apoptotic cells were observed after RANK-Fc treatments (Fig. 2B-C). However, limiting dilution assays (LDA) revealed that tumor cells pre-treated with RANK-Fc at passage 1 showed a 10-fold decrease in tumor-initiating ability whereas RANK-Fc treatment only at passage 2 did not significantly change tumor-initiating cell frequency (Fig. 2D). Concomitantly, the ability to form secondary tumorspheres was significantly impaired in cells derived from the RANK-Fc-pre-treated pool (Fig. 2E), consistent with a reduction in CSC population (19). These results demonstrate that pre-treatment with RANK-Fc reduces tumor-initiating ability, and suggests that in clinics, RANKL inhibition may reduce the risk of relapse by depleting the population of CSCs.

Pharmacological inhibition of RANK signaling induces lactogenic differentiation of tumor cells

To investigate the molecular mechanism underlying the reduction in tumor initiating ability, we analyzed global gene expression profiles from all RANK-Fc treatment arms. Genes induced by RANK-Fc included milk proteins such as *Pip*, caseins, *Wap,* or *Lpl* which are expressed during differentiation of mammary cells into milk-secreting alveoli (21) and multiple members of the secretoglobin family (*Scgb1b27, Scgb1b30, Scgb2b2*)

which are associated with differentiation and low risk of relapse in human breast cancer (3, 27) (Table S1 and Fig. 3A). In fact, genes up-regulated during lactation (21) were significantly over-expressed in the RANK-Fc-treated tumors (Fig. 3A-B). Up-regulation of *Csn2*, *Pip*, *Scgb1b27* and *Scgb2b27* mRNA was confirmed in the RANK-Fc -treated tumors (Fig. 3C). Immunostaining with an anti-milk antibody confirmed that RANKL inhibition induced differentiation of late-adenocarcinoma cells into milk secreting cells (Fig. 3D). Conversely, tumor acini cultured with RANKL showed lower *Csn2, Pip* and *Scgb2b27* expression (Fig. 3E), in correlation with the reduced milk protein found in vivo (Fig. 1F-G). These results demonstrate that pharmacological inhibition of RANK signaling in PyMT tumor-bearing mice promotes tumor cells differentiation into an apocrine, milk-secreting phenotype that mimics mammary lactogenesis, concomitantly with the reduction in tumor initiating ability.

RANK deletion increases tumor latency, decreases tumor incidence and impairs lung metastasis in MMTV-PyMT mice

Genetic deletion of RANK in the MMTV-PyMT background significantly delayed tumor onset and reduced tumor incidence (Fig. 4A-B, S4A). In accordance with their multifocal origin (24), PyMT;$RANK^{+/+}$ palpable lesions showed multiple stages of tumor progression whereas one predominant stage was found throughout the whole PyMT;$RANK^{-/-}$ palpable mass (Fig. S4B-C). Accordingly, the number of preneoplasic lesions quantified in mammary gland whole mounts was significantly reduced in PyMT;$RANK^{-/-}$ compared with control mice (Fig. 4C). PyMT;$RANK^{-/-}$ lesions contained extensive areas of early and/or late carcinoma indicating that tumors can progress to the invasive stage in the absence of RANK. However, most of PyMT;$RANK^{-/-}$ mice were devoid of lung metastasis, while all

PyMT;RANK$^{+/+}$ mice with early/late carcinomas developed lung metastasis, and several showed 30-200 metastatic foci per lung (Fig. 4D). Thus, RANK deletion increases tumor latency, decreases tumor incidence and impairs lung metastasis in the MMTV-PyMT tumor-prone model.

RANK loss in tumor cells depletes the tumor and metastasis-initiating cell pools and increases apoptosis and sensitivity to docetaxel

To rule out the progesterone/RANKL-mediated effects acting in early tumorigenesis (7) and the influence of the RANK-null microenvironment (17), PyMT;RANK$^{-/-}$ and PyMT;RANK$^{+/+}$ tumors cells, isolated from established carcinomas were orthotopically implanted in syngeneic WT females. PyMT;RANK$^{-/-}$ tumor cells showed a significantly longer latency to tumor formation than did PyMT;RANK$^{+/+}$ tumor cells, indicating a tumor cell autonomous defect (Fig. 5A). Longer latency was also observed when PyMT;RANK$^{+/+}$ tumor cells were implanted in RANK null mice compared with WT, but no synergic effect after implantation of PyMT;RANK$^{-/-}$ in RANK null hosts was found (Fig. 5A).

PyMT;RANK$^{-/-}$ tumors growing in WT hosts contained more apoptotic cells and extensive non-viable areas relative to PyMT;RANK$^{+/+}$ tumors (Fig. 5B-C). No significant differences in tumor cell survival were observed when the same tumor, either PyMT;RANK+/+ or PyMT;RANK-/-, was implanted on WT and RANK null hosts supporting a tumor cell intrinsic mechanism (Fig. 5C). This demonstrates that tumor cell survival is impaired in the absence of RANK, which may contribute to the delayed tumor formation observed. Moreover, the absence of RANK on tumor cells sensitized tumors to docetaxel (Fig. 5D).

Next, we aimed to determine whether loss of RANK signaling exclusively on tumor cells reduced the CSC pool as observed after RANKL inhibition. PyMT;RANK$^{-/-}$ tumor cells

gave rise to less tumorspheres than controls, independently of the initial host (Fig. 5E), highlighting an extenuation of a self-renewal capability that is tumor cell-autonomous. LDA in WT hosts also revealed a significant reduction in the frequency of tumor-initiating cells (TICs) in the absence of RANK (Fig. 5F). PyMT;$RANK^{+/+}$ tumor cells efficiently colonized the lung of *Foxn1*^{nu} mice and abundant metastatic foci were found (Fig. 5G-H). Strikingly, in the PyMT;$RANK^{-/-}$ pool a 10-fold decrease in the frequency of metastasis-initiating cells (MICs) was observed with very few metastatic foci (Fig. 5G-H), implying that RANK expression in tumor cells is determinant for metastasis. Thus, RANK loss in advanced adenocarcinomas depleted the pool of tumor and metastasis-initiating cells, decreased survival and sensitized tumors to docetaxel.

RANKL negatively regulates the Ap2 transcription factors, drivers of the luminal differentiation, and induces the expression of Rspo1.

To further understand the molecular mechanism underlying tumor cell differentiation after RANKL inhibition we focused on genes specifically induced in tumors that received RANK-Fc treatment at passage 1 such as *Tfap2b* (Table S1). The AP2 transcription factor family is a set of retinoic acid inducible genes that governs the luminal epithelial phenotype in mammary development and carcinogenesis (28, 29) and whose expression is associated with survival (30, 31). Consistent with a tumor cell- luminal differentiation phenotype GSEA analyses of the genes that characterize mammary differentiation hierarchy (20), revealed that the mature luminal up-regulated set and the mammary stem cell down-regulated set, were over-expressed on the RANK-Fc treated tumors (Fig. 6A). *Spdef*, which also promotes luminal differentiation (32) was the top gene in these associations (Fig 6A). Genes up-regulated by TFAP2C in human breast cancer cells (22) were significantly

overexpressed in RANK-Fc-treated tumors (Fig 6B). Moreover, an increase in *Tfap2a* and *Tfap2b* was observed in the RANK null mammary epithelia and RANKL treatment significantly reduced the *Tfap2a, Tfap2b* and *Tfap2c* mRNA expression in tumor cultures of PyMT cells (Fig. 6C-D, G).

Gene expression analysis in the pre-RANK-Fc treated tumors confirmed upregulation of *Tfap2b*, the luminal genes Sp*def* and *Fbp1* and *cdkn1a/p21* (known to be induced by Tfap2) (29) and downregulation of the basal genes *p63*, *Krt14*. No significant changes were detected between groups in *Krt8, Foxa1, Gata3*, *Esr1, Elf5* and *Rspo1* (Fig. 6E). Higher levels of *Tfap2b, Tfap2c* and *p21* and lower levels of *Krt14* and *Rspo1* were found in PyMT;RANK-/- tumor cells isolated from transplants as compared to controls (Fig. 6F). R-spondin1, *Rspo1*, a Wnt agonist that has been shown to be expressed on luminal progenitors and mediate RANK-driven expansion of mammary progenitors in the healthy gland (33, 34) was strongly induced by RANKL on PyMT acini cultures (Fig. 6G). Tfap2b overexpressing and knock-down PyMT tumor cells were obtained as little is known about the specific role of Tfap2b on mammary tumors (Fig S5A-B). Gene expression analyses confirmed that *Spdef* was positively regulated by Tfap2b (Fig. S5C). Analyses of PyMT tumor acini cultured for 2 weeks revealed that RANKL led to an increase on acini size irrespectively of Tfap2b expression (Fig. S6). However, in Tfap2b overexpressing PyMT acini treated with RANKL, *Rspo1* mRNA expression was 30% lower than in RANKL-treated control acini. Conversely, in shTfap2b PyMT acini treated with RANKL, *Rspo1* expression was 50% higher than in controls, demonstrating that Tfap2b interfered with RANKL-driven increase in *Rspo1* (Fig 6H). *Rspo1* expression decreased, whereas *Tfap2b* and *Spdef* expression increased in PyMT tumor cells infected with shRANK, further supporting that RANK pathway negatively regulates luminal differentiation (Fig. S5D).

To investigate the clinical relevance of TFAP2B we analyzed an expression dataset from lymph-node negative breast cancer patients that developed distant metastasis (35). The expression of *TFAP2B* was found to be significantly associated with the absence of distant metastasis: Cox regression hazard ratio (HR) = 0.25, 95% confidence interval (CI) = 0.11 – 0.57, p=0.001 (Fig 6I). Similar results were observed in tumors with a luminal phenotype (ER+): HR = 0.24, (0.09 – 0.63), p=0.004 and the same trend for (ER-) tumors: HR = 0.24, (0.04-1.29) p= 0.09. Consistent with the proposed cancer-promoting role for enhanced RANK signaling, associations with relapse free were observed for *TNFRSF11B* (OPG*),* the canonical negative regulator of the RANK pathway: HR = 0.49, (0.31 – 0.78), p=0.002 (Fig. 6I); in luminal tumors (ER+): HR =0.33, (0.17 – 0.62), p=0.0006. Accordingly, *TFAP2B* and *TNFRSF11B* were found to be significantly co-expressed (Pearson's correlation coefficient =0.14, p=0.018). Together these data indicate that RANKL inhibition leads to tumor differentiation, metastasis impairment and good prognosis.

RANK signaling inhibition depletes the pool of Sca1- tumor initiating cells

Next, we aimed to identify the CSC population regulated by RANK in our models, which remains elusive in the MMTV-PyMT model (36-38). The levels of CD49f, CD49b, CD61 and CD90 within epithelial cells were comparable for all RANK-Fc treatment arms; in contrast, Sca1+/hi cells were more abundant in tumors pretreated with RANK-Fc, which show a lower tumor initiating ability (Fig. 7A, B). In the normal mammary gland Sca1+ identifies a population enriched in ER+/PR luminal mature cells (37). However, we could not detect an increase in PR+ cells after RANK-Fc treatment (Fig. 7C). Similarly, an increase in the Sca1+/hi population, but none of the other markers, was found in PyMT;RANK$^{-/-}$ tumors as compared to controls (Fig 7D). Secondary tumorspheres of Sca1-

/lo tumor cells were larger and five times more numerous as those of Sca1+/hi cells (Fig. 7E-F). Strikingly, LDA assays revealed the TIC frequency is significantly enhanced by 200-fold in Sca1-/lo compared with Sca1+/hi tumor cells (Fig. 7G), indicating that the Sca1-/lo population is enriched in CSCs. Altogether these results demonstrated that RANK loss or RANKL inhibition reduced the frequency of the Sca1-/lo CSC population.

DISCUSSION

The work presented here reveals a central role of RANK signaling promoting recurrence and metastasis in aggressive breast tumors, providing a rationale for additional therapeutic applications of RANK inhibitors beyond its current use for the management of skeletal related events. We found that constitutive deletion of RANK in MMTV-PyMT mice increases tumor latency and decreases tumor and lung metastasis incidence, as observed in MMTV-neu mice upon RANK-Fc preventive treatment (7), reinforcing the role of RANK signaling in early stages of tumorigenesis (8).

Our previous data showed that enhanced RANK activation promotes stemness in human and mouse mammary epithelia leading to the accumulation of MaSC and progenitors (11, 12, 39). Importantly, now we demonstrate that inhibition of RANK signaling reduces CSC in invasive mammary tumors decreasing recurrence and metastasis, and induces tumor cell differentiation. LDA assays aim to mimic occult disease that remains in breast cancer patients after surgery. Our results suggest that neoadjuvant RANKL inhibition may be more efficient in reducing recurrence and metastasis than adjuvant treatment, as a significant reduction in the CSC population was observed on tumors treated at passage 1. Along with our previous data demonstrating that over-activation of RANK signaling at midgestation disrupts lactogenesis (12, 39), these results suggest that RANK signaling regulates the balance between self-renewal and differentiation not only during mammary gland development but also in breast adenocarcinomas.

The impaired tumor and metastasis initiation ability observed in RANK null tumor cells growing in WT hosts demonstrates that tumor cell intrinsic mechanisms mediate the observed reduction in CSC. However, we cannot discard that tumor cell extrinsic

mechanisms induced by RANK signaling inhibition in the microenvironment, can also contribute to reduce recurrence (40).

Mechanistically, we demonstrate that RANK signaling negatively regulates the AP2 transcription factor family which can mediate retinoic acid responsiveness (41, 42). TFAP2A functions as a tumor suppressor in several solid tumors including breast cancer (43, 44). Overexpression of Tfap2a and Tfap2c mimics the mammary phenotype of RANK null mice (5, 45, 46). Tfap2a and Tfap2c maintain the luminal phenotype (28, 29) and negative regulate cancer stem cell markers (28). Although little is known about TFAP2B in mammary epithelia our results suggest that, similarly to other members of the family, TFAP2B promotes luminal differentiation and is associated with good prognosis. The positive correlation between the RANKL inhibitor, *OPG*, and *TFAP2B* expression in human breast tumors and their association with metastasis free phenotype support the clinical implication of our findings.

Although, enhanced Tfap2b expression alone cannot prevent RANKL-driven increased in acinar size it interferes with the induction of the Wnt agonist Rspo1. Rspo1 together with Wnt4 promote MaSC self renewal and Rspo1 rescue some of the mammary developmental defects in RANK null epithelia (33, 34). Similarly to our previous results on mammary epithelial cells at midgestation where RANKL induces the expression of Rspo1, leads to the expansion of basal and bipotent cells and prevents lactogenic differentiation (39), we now observe that on PyMT tumor acini, RANK pathway also enhances Rspo1 and interferes with differentiation. Our results evidence a complex regulatory loop between RANK, Tfap2 and Rspo1 underlying the reduction in the CSC pool observed upon RANK pathway inhibition (Fig. 7H), but further experiments will be required to clarify their contribution to the protumorigenic role of RANK in cancer. Sca-1/Ly6A is found in the luminal

differentiated ER+/PR+ cell cluster and according to our data it is likely to be induced by Tfap2, whereas Rspo1 is expressed on luminal Sca1- progenitor cells (33, 34). The decrease in Sca1- cells upon RANK loss or inhibition and their enhanced mammosphere-forming and tumor-initiating potential demonstrate that this population is enriched in CSCs in the PyMT tumors, as shown in the MMTV-wnt model (47). A negative regulation of Sca1+ by RANK has been observed during mammary gland development (12, 34). The relevance of Sca1/Ly6a as a CSC marker in human luminal adenocarcinomas deserves further investigation.

Mortality in breast cancer is due to tumor recurrence and metastasis, which is driven by surviving CSC. RANKL inhibitors, although unable to reduce tumor growth, can be used as differentiation therapy of CSC (Figure 7H). Moreover, RANK null tumor cells are more susceptible to taxanes than RANK expressing tumor cells, supporting the use of neoadjuvant RANKL inhibitors in the clinical setting to reduce the frequency of tumor relapse and metastasis and to increase sensitivity to chemotherapy. FDA-approved RANKL inhibitors are currently used in clinic for the management of skeletal related events therefore patients may quickly benefit from this therapeutic strategy to combat advanced breast cancer.

ACKNOWLEDGEMENTS

We thank L Alcaraz and D Amoros (Bioarray) for microarray analyses, NE Hynes, M. Glukhova's group, M Bentires-Alj, S Duss and K Jin for sharing protocols and reagents, G. Boigues, A. Villanueva, E Castaño and the IDIBELL animal facility for their technical assistance.

REFERENCES

1. Li, X., Lewis, M. T., Huang, J., Gutierrez, C., Osborne, C. K., Wu, M. F., Hilsenbeck, S. G., Pavlick, A., Zhang, X., Chamness, G. C., Wong, H., Rosen, J., and Chang, J. C. Intrinsic resistance of tumorigenic breast cancer cells to chemotherapy. J Natl Cancer Inst, *100:* 672-679, 2008.
2. Tallman, M. S., Andersen, J. W., Schiffer, C. A., Appelbaum, F. R., Feusner, J. H., Ogden, A., Shepherd, L., Willman, C., Bloomfield, C. D., Rowe, J. M., and Wiernik, P. H. All-trans-retinoic acid in acute promyelocytic leukemia. N Engl J Med, *337:* 1021-1028, 1997.
3. Dontu, G., Abdallah, W. M., Foley, J. M., Jackson, K. W., Clarke, M. F., Kawamura, M. J., and Wicha, M. S. In vitro propagation and transcriptional profiling of human mammary stem/progenitor cells. Genes Dev, *17:* 1253-1270, 2003.
4. Beleut, M., Rajaram, R. D., Caikovski, M., Ayyanan, A., Germano, D., Choi, Y., Schneider, P., and Brisken, C. Two distinct mechanisms underlie progesterone-induced proliferation in the mammary gland. Proc Natl Acad Sci U S A, *107:* 2989-2994, 2010.
5. Fata, J. E., Kong, Y. Y., Li, J., Sasaki, T., Irie-Sasaki, J., Moorehead, R. A., Elliott, R., Scully, S., Voura, E. B., Lacey, D. L., Boyle, W. J., Khokha, R., and Penninger, J. M. The osteoclast differentiation factor osteoprotegerin-ligand is essential for mammary gland development. Cell, *103:* 41-50, 2000.
6. Tanos T, S. G., Echeverria PC, Ayyanan A, Gutierrez M, Delaloye JF, Raffoul W, Fiche M, Dougall W, Schneider P, Yalcin-Ozuysal O, Brisken C Progesterone/RANKL is a major regulatory axis in the human breast. Sci Transl Med, *5:* 182ra155, 2013.
7. Gonzalez-Suarez, E., Jacob, A. P., Jones, J., Miller, R., Roudier-Meyer, M. P., Erwert, R., Pinkas, J., Branstetter, D., and Dougall, W. C. RANK ligand mediates progestin-induced mammary epithelial proliferation and carcinogenesis. Nature, *468:* 103-107, 2010.
8. Gonzalez-Suarez, E. RANKL inhibition: a promising novel strategy for breast cancer treatment. Clin Transl Oncol, *13:* 222-228, 2011.
9. Schramek, D., Leibbrandt, A., Sigl, V., Kenner, L., Pospisilik, J. A., Lee, H. J., Hanada, R., Joshi, P. A., Aliprantis, A., Glimcher, L., Pasparakis, M., Khokha, R., Ormandy, C. J., Widschwendter, M., Schett, G., and Penninger, J. M. Osteoclast differentiation factor RANKL controls development of progestin-driven mammary cancer. Nature, *468:* 98-102, 2010.
10. Gonzalez-Suarez, E., Branstetter, D., Armstrong, A., Dinh, H., Blumberg, H., and Dougall, W. C. RANK overexpression in transgenic mice with mouse mammary tumor virus promoter-controlled RANK increases proliferation and impairs alveolar differentiation in the mammary epithelia and disrupts lumen formation in cultured epithelial acini. Mol Cell Biol, *27:* 1442-1454, 2007.
11. Palafox, M., Ferrer, I., Pellegrini, P., Vila, S., Hernandez-Ortega, S., Urruticoechea, A., Climent, F., Soler, M. T., Munoz, P., Vinals, F., Tometsko, M., Branstetter, D., Dougall, W. C., and Gonzalez-Suarez, E. RANK induces epithelial-mesenchymal transition and stemness in human mammary epithelial cells and promotes tumorigenesis and metastasis. Cancer Res, *72:* 2879-2888, 2012.

12. Pellegrini, P., Cordero, A., Gallego, M. I., Dougall, W. C., Purificacion, M., Pujana, M. A., and Gonzalez-Suarez, E. Constitutive activation of RANK disrupts mammary cell fate leading to tumorigenesis. Stem Cells, *31:* 1954-1965, 2013.
13. Pfitzner, B. M., Branstetter, D., Loibl, S., Denkert, C., Lederer, B., Schmitt, W. D., Dombrowski, F., Werner, M., Rudiger, T., Dougall, W. C., and von Minckwitz, G. RANK expression as a prognostic and predictive marker in breast cancer. Breast Cancer Res Treat, *145:* 307-315, 2014.
14. Santini, D., Schiavon, G., Vincenzi, B., Gaeta, L., Pantano, F., Russo, A., Ortega, C., Porta, C., Galluzzo, S., Armento, G., La Verde, N., Caroti, C., Treilleux, I., Ruggiero, A., Perrone, G., Addeo, R., Clezardin, P., Muda, A. O., and Tonini, G. Receptor activator of NF-kB (RANK) expression in primary tumors associates with bone metastasis occurrence in breast cancer patients. PLoS One, *6:* e19234, 2011.
15. Guy, C. T., Cardiff, R. D., and Muller, W. J. Induction of mammary tumors by expression of polyomavirus middle T oncogene: a transgenic mouse model for metastatic disease. Mol Cell Biol, *12:* 954-961, 1992.
16. Maglione, J. E., Moghanaki, D., Young, L. J., Manner, C. K., Ellies, L. G., Joseph, S. O., Nicholson, B., Cardiff, R. D., and MacLeod, C. L. Transgenic Polyoma middle-T mice model premalignant mammary disease. Cancer Res, *61:* 8298-8305, 2001.
17. Dougall, W. C., Glaccum, M., Charrier, K., Rohrbach, K., Brasel, K., De Smedt, T., Daro, E., Smith, J., Tometsko, M. E., Maliszewski, C. R., Armstrong, A., Shen, V., Bain, S., Cosman, D., Anderson, D., Morrissey, P. J., Peschon, J. J., and Schuh, J. RANK is essential for osteoclast and lymph node development. Genes Dev, *13:* 2412-2424, 1999.
18. Smalley, M. J. Isolation, culture and analysis of mouse mammary epithelial cells. Methods Mol Biol, *633:* 139-170, 2010.
19. Dontu, G. and Wicha, M. S. Survival of mammary stem cells in suspension culture: implications for stem cell biology and neoplasia. J Mammary Gland Biol Neoplasia, *10:* 75-86, 2005.
20. Lim, E., Wu, D., Pal, B., Bouras, T., Asselin-Labat, M. L., Vaillant, F., Yagita, H., Lindeman, G. J., Smyth, G. K., and Visvader, J. E. Transcriptome analyses of mouse and human mammary cell subpopulations reveal multiple conserved genes and pathways. Breast Cancer Res, *12:* R21, 2010.
21. Anderson, S. M., Rudolph, M. C., McManaman, J. L., and Neville, M. C. Key stages in mammary gland development. Secretory activation in the mammary gland: it's not just about milk protein synthesis! Breast Cancer Res, *9:* 204, 2007.
22. Woodfield, G. W., Chen, Y., Bair, T. B., Domann, F. E., and Weigel, R. J. Identification of primary gene targets of TFAP2C in hormone responsive breast carcinoma cells. Genes Chromosomes Cancer, *49:* 948-962, 2010.
23. Hu, Y. and Smyth, G. K. ELDA: extreme limiting dilution analysis for comparing depleted and enriched populations in stem cell and other assays. J Immunol Methods, *347:* 70-78, 2009.
24. Lin, E. Y., Jones, J. G., Li, P., Zhu, L., Whitney, K. D., Muller, W. J., and Pollard, J. W. Progression to malignancy in the polyoma middle T oncoprotein mouse breast cancer model provides a reliable model for human diseases. Am J Pathol, *163:* 2113-2126, 2003.

25. Barcellos-Hoff, M. H., Aggeler, J., Ram, T. G., and Bissell, M. J. Functional differentiation and alveolar morphogenesis of primary mammary cultures on reconstituted basement membrane. Development, *105:* 223-235, 1989.
26. Lee, G. Y., Kenny, P. A., Lee, E. H., and Bissell, M. J. Three-dimensional culture models of normal and malignant breast epithelial cells. Nat Methods, *4:* 359-365, 2007.
27. Span, P. N., Waanders, E., Manders, P., Heuvel, J. J., Foekens, J. A., Watson, M. A., Beex, L. V., and Sweep, F. C. Mammaglobin is associated with low-grade, steroid receptor-positive breast tumors from postmenopausal patients, and has independent prognostic value for relapse-free survival time. J Clin Oncol, *22:* 691-698, 2004.
28. Bogachek, M. V., Chen, Y., Kulak, M. V., Woodfield, G. W., Cyr, A. R., Park, J. M., Spanheimer, P. M., Li, Y., Li, T., and Weigel, R. J. Sumoylation pathway is required to maintain the basal breast cancer subtype. Cancer Cell, *25:* 748-761, 2014.
29. Cyr, A. R., Kulak, M. V., Park, J. M., Bogachek, M. V., Spanheimer, P. M., Woodfield, G. W., White-Baer, L. S., O'Malley, Y. Q., Sugg, S. L., Olivier, A. K., Zhang, W., Domann, F. E., and Weigel, R. J. TFAP2C governs the luminal epithelial phenotype in mammary development and carcinogenesis. Oncogene, *34:* 436-444, 2014.
30. Bar-Eli, M. Role of AP-2 in tumor growth and metastasis of human melanoma. Cancer Metastasis Rev, *18:* 377-385, 1999.
31. Gee, J. M., Robertson, J. F., Ellis, I. O., Nicholson, R. I., and Hurst, H. C. Immunohistochemical analysis reveals a tumour suppressor-like role for the transcription factor AP-2 in invasive breast cancer. J Pathol, *189:* 514-520, 1999.
32. Buchwalter, G., Hickey, M. M., Cromer, A., Selfors, L. M., Gunawardane, R. N., Frishman, J., Jeselsohn, R., Lim, E., Chi, D., Fu, X., Schiff, R., Brown, M., and Brugge, J. S. PDEF promotes luminal differentiation and acts as a survival factor for ER-positive breast cancer cells. Cancer Cell, *23:* 753-767, 2013.
33. Cai, C., Yu, Q. C., Jiang, W., Liu, W., Song, W., Yu, H., Zhang, L., Yang, Y., and Zeng, Y. A. R-spondin1 is a novel hormone mediator for mammary stem cell self-renewal. Genes Dev, *28:* 2205-2218, 2014.
34. Joshi, P. A., Waterhouse, P. D., Kannan, N., Narala, S., Fang, H., Di Grappa, M. A., Jackson, H. W., Penninger, J. M., Eaves, C., and Khokha, R. RANK Signaling Amplifies WNT-Responsive Mammary Progenitors through R-SPONDIN1. Stem Cell Reports, *5:* 31-44, 2015.
35. Wang, Y., Klijn, J. G., Zhang, Y., Sieuwerts, A. M., Look, M. P., Yang, F., Talantov, D., Timmermans, M., Meijer-van Gelder, M. E., Yu, J., Jatkoe, T., Berns, E. M., Atkins, D., and Foekens, J. A. Gene-expression profiles to predict distant metastasis of lymph-node-negative primary breast cancer. Lancet, *365:* 671-679, 2005.
36. Malanchi I, S.-M. A., Susanto E, Peng H, Lehr HA, Delaloye JF, Huelsken J. Interactions between cancer stem cells and their niche govern metastatic colonization. Nature, *481:* 85-89, 2011.
37. Sleeman, K. E., Kendrick, H., Robertson, D., Isacke, C. M., Ashworth, A., and Smalley, M. J. Dissociation of estrogen receptor expression and in vivo stem cell activity in the mammary gland. J Cell Biol, *176:* 19-26, 2007.

38. Vaillant, F., Asselin-Labat, M. L., Shackleton, M., Forrest, N. C., Lindeman, G. J., and Visvader, J. E. The mammary progenitor marker CD61/beta3 integrin identifies cancer stem cells in mouse models of mammary tumorigenesis. Cancer Res, *68:* 7711-7717, 2008.
39. Cordero, A., Pellegrini, P., Sanz-Moreno, A., Trinidad, E. M., Serra-Musach, J., Deshpande, C., Dougall, W. C., Pujana, M. A., and Gonzalez-Suarez, E. Rankl Impairs Lactogenic Differentiation Through Inhibition of the Prolactin/Stat5 Pathway at Midgestation. Stem Cells, *34:* 1027-1039, 2016.
40. Gonzalez-Suarez, E. and Sanz-Moreno, A. RANK as a therapeutic target in cancer. Febs J, *283:* 2018-2033, 2016.
41. Bosher, J. M., Totty, N. F., Hsuan, J. J., Williams, T., and Hurst, H. C. A family of AP-2 proteins regulates c-erbB-2 expression in mammary carcinoma. Oncogene, *13:* 1701-1707, 1996.
42. McPherson, L. A., Woodfield, G. W., and Weigel, R. J. AP2 transcription factors regulate expression of CRABPII in hormone responsive breast carcinoma. J Surg Res, *138:* 71-78, 2007.
43. McPherson, L. A., Loktev, A. V., and Weigel, R. J. Tumor suppressor activity of AP2alpha mediated through a direct interaction with p53. J Biol Chem, *277:* 45028-45033, 2002.
44. Scibetta, A. G., Wong, P. P., Chan, K. V., Canosa, M., and Hurst, H. C. Dual association by TFAP2A during activation of the p21cip/CDKN1A promoter. Cell Cycle, *9:* 4525-4532, 2010.
45. Jager, R., Werling, U., Rimpf, S., Jacob, A., and Schorle, H. Transcription factor AP-2gamma stimulates proliferation and apoptosis and impairs differentiation in a transgenic model. Mol Cancer Res, *1:* 921-929, 2003.
46. Zhang, J., Brewer, S., Huang, J., and Williams, T. Overexpression of transcription factor AP-2alpha suppresses mammary gland growth and morphogenesis. Dev Biol, *256:* 127-145, 2003.
47. Batts, T. D., Machado, H. L., Zhang, Y., Creighton, C. J., Li, Y., and Rosen, J. M. Stem cell antigen-1 (sca-1) regulates mammary tumor development and cell migration. PLoS One, *6:* e27841, 2011.

FIGURE LEGENDS

Figure 1. RANKL decreases MMTV-PyMT tumor cell differentiation

A. Representative images of RANK and RANKL protein expression. Note that in carcinomas RANKL is not expressed in tumor cells but in tumor infiltrating lymphocytes.

B. *Rank* and *Rankl* mRNA expression relative to β-actin in 7 WT, 8 MMTV-PyMT tumors and 3 draining lymph nodes of MMTV-PyMT tumor-bearing mice.

C. *Rankl* mRNA expression relative to *Rpl38* in FACS-sorted (Fig. S2) tumor cells (TUM) CD45-, macrophages (TAM) CD45+CD11b+F4/80+Gr1-, CD4+ and CD8+ T lymphocytes CD45+CD11b-CD3+CD4+ or CD8 from four MMTV-PyMT tumors.

D. Schematic overview of short-term (2 weeks) RANKL treatment in MMTV-PyMT tumor-bearing females.

E. Tumor volume normalized to the first day of treatment of 5 MMTV-PyMT mice undergoing RANKL treatment and controls.

F. Percentage of secretory areas relative to total tumor area in (3-5) MMTV-PyMT primary tumors after RANKL treatment.

G. Representative images of H&E and milk protein staining in MMTV-PyMT primary tumors.

B, E, F: Mean, SEM and t test probabilities are shown. (*, $0.01<P<0.05$; **, $0.001<P<0.01$; ***, $0.001<P<0.0001$).

Figure 2. Inhibition of RANK signaling depletes the pool of MMTV-PyMT tumor-initiating cells.

A. Schematic overview of RANK-Fc treatments in orthotopic MMTV-PyMT tumors. One million cells isolated from one MMTV-PyMT carcinoma were orthotopically injected into

syngeneic WT mice (FVB), which were randomized 1:1 for RANK-Fc (10 mg/kg, three times per week, 4 weeks) or mock treatment starting 24h later (passage 1). Cells isolated from 3 tumor of each treatment arm were pooled and orthotopically injected into WT (passage 2) mice in limiting dilutions and randomized 1:1 for additional RANK-Fc or mock treatment (2 weeks). Total number of tumors was scored after 26 weeks.

B. Tumor growth of passage 1 tumors.

C. Percentage of positive cleaved caspase 3 cells in passage 2 tumors.

D. Tumor-initiating cell frequencies (with confidence intervals) chi-square values and associated probabilities.

E. Number of secondary tumorspheres formed by RANK-Fc-treated MMTV-PyMT tumors. Each bar represents data from four tumors plated in triplicates. Mean, SEM and t-test statistics are shown (*, $0.01 < P < 0.05$).

Figure 3. RANKL inhibition induces differentiation of tumor cells into milk secreting cells.

A. Expression profile in mammary gland development of differentially expressed genes between RANK-Fc treated tumor and controls (21). Genes further validated by RT-PCR are shown in red.

B. GSEA graphical output for the association between lactation over-expressed genes and RANK-Fc treatment. The top genes contributing to this association are listed.

C. mRNA expression levels of indicated genes relative to *HPRT*. Each bar is representative of three tumors.

D. Representative images of milk staining in RANK-Fc (passage 1 & 2) treated tumors.

E. Fold change of mRNA expression levels of indicated genes in RANKL treated acinar cultures of MMTV-PyMT tumor cells relative to untreated controls. Three tumors were analyzed.

B, E: Mean, SEM, and t test p values are shown (*, $0.01 < P < 0.05$)

Figure 4. **Constitutive deletion of RANK increases tumor latency, decreases tumor incidence, and prevents lung metastasis of MMTV-PyMT tumors.**

A. Kinetics of palpable tumor onset with age in 18 PyMT;$RANK^{+/+}$ and 10 PyMT;$RANK^{-/-}$ mice. Log-rank test (****, $P<0.0001$).

B. Number of palpable lesions detected at necropsy in 17 PyMT;$RANK^{+/+}$ and 10 PyMT;$RANK^{-/-}$ mice.

C. Number of preneoplasic regions per mammary gland detected in mammary whole mounts of 9 PyMT;$RANK^{+/+}$ and 5 PyMT;$RANK^{-/-}$ females 13-22 weeks-old. Each dot represents one mammary gland.

D. Percentage of PyMT;$RANK^{+/+}$ (n=6) and PyMT;$RANK^{-/-}$ (n=7) females with lung metastasis. The total number of metastatic foci per mouse is indicated. Chisq:=6.96, as calculated by contingency 2x2, p=0.01.

B, C: Mean, SEM, and t test p values are shown (*, $0.01 < P < 0.05$).

Figure 5. RANK-null tumors contain fewer tumor and metastasis-initiating cells, have enhanced apoptosis and are more sensitive to docetaxel.

A. Latency to tumor formation of PyMT;$RANK^{+/+}$ and PyMT;$RANK^{-/-}$ tumor cells orthotopically implanted in WT and $RANK^{-/-}$ syngeneic mice. 22 tumors from each group were quantified.

B. Representative pictures of cleaved caspase 3 staining in transplants..

C. Percentage of non-viable areas versus total tumor area and cleaved caspase 3-positive nuclei in transplants. Each dot represents one tumor.

D. Relative tumor volume (length*width/100) of PyMT;RANK$^{+/+}$ and PyMT;RANK$^{-/-}$ tumors treated with docetaxel (25 mg/kg) twice per week. # indicate docetaxel doses.

E. Number of tertiary tumorspheres. Each bar represents four tumors.

F-G. Tumor-initiating (F) and metastasis-initiating frequencies (G) (with confidence intervals) and chi-square values. Cells from two tumors per genotype were pooled for injections and metastasis was scored after 8 weeks.

H. Absolute number of lung metastasis. Each dot represents the lung of one mouse.

A, E, H: Mean, SEM and t test (F test for H) probabilities are shown (*, 0.01<P<0.05; **, 0.001 <P<0.01; ***, 0.001<P <0.0001; ****, P<0.0001).

Figure 6. RANK loss or inhibition induces the expression of AP2 transcription factors and reduces Rspo1.

A, B. GSEA graphical outputs for the association between mammary mature luminal (up-regulated genes) and stem (down-regulated genes) cells gene sets (A) and TFAP2C up-regulated genes sets in human breast cancer (B) and RANK-Fc treatment. The top genes contributing to the association are listed.

C. Fold changes in mRNA expression of indicated genes in PyMT tumor cultures treated with RANKL for 24h relative to untreated cultures. Each bar is representative of three tumors.

D. mRNA expression levels of indicated genes relative to *Krt8* in PyMT RANK+/+ and PyMT;RANK-/- mammary glands. Each bar is representative of three mammary glands.

E. Fold changes in mRNA expression of indicated genes in RANK-Fc treated PyMT tumors at passage 1 relative to expression in the other treatment arms. Each bar is representative of six tumors.

F. Fold changes in mRNA expression of indicated genes in PyMT;RANK-/- relative to expression in PyMT;RANK+/+ sorted tumor cells. Each bar is representative of three-four independent tumors.

G: Fold change of *Rspo1* and *Tfap2b* mRNA expression levels in PyMT acini tumor acini cultured with RANKL for 3 and 14 days relative to untreated cultures.

H. Relative induction of *Rspo1* mRNA expression upon in Tfap2b knockdown or overexpressing PyMT tumor acini cultured with RANKL for 14 days relative to the induction in RANKL treated controls (normalized as 100%). Induction of *Rspo1* mRNA in shRANK-698 is included.

I. Association between *TFAP2B* and *TNFRSF11B* tumor expression and distant metastasis in lymph-node negative breast cancer patients (GSE2034). Graphs show the proportion of distant metastasis-free patients over time (months) and stratified according to the first (low expression) or the third (high expression) tertiles.

C, D, E, F: Mean, SEM and t-test statistics are shown. (*, $0.01 < P < 0.05$; **, $0.001 < P < 0.01$; ***, $0.001 < P < 0.0001$; ****, $P<0.0001$)

Figure 7. RANK-Fc pre-treatment reduces the Sca1- tumor cell population.

A. Frequency of the indicated populations within tumor CD45-CD31-CD24+ cells. Each bar represents data from four mice in two independent experiments.

B. Representative histograms of Sca1+/hi and Sca1-/lo populations.

C. Representative images of PR immunostaining.

D. Frequency of the indicated populations within tumor cell transplants. Each bar is representative of 3-5 tumors.

E, F. Representative images (E) and number (F) of tumorspheres derived from FACS-sorted Sca1+/hi and Sca1- tumor cells. Each bar is representative of two tumors quantified in triplicates.

G. Tumor-initiating frequency (with confidence intervals) chi-square values and associated probabilities.

H. Graphical abstract indicating the multiple effects observed after therapeutic inhibition of RANK pathway in MMTV-PyMT tumors.

A, D, F: Mean, SEM and t-test statistics are shown (**, $0.001 < P < 0.01$).

Figure 1

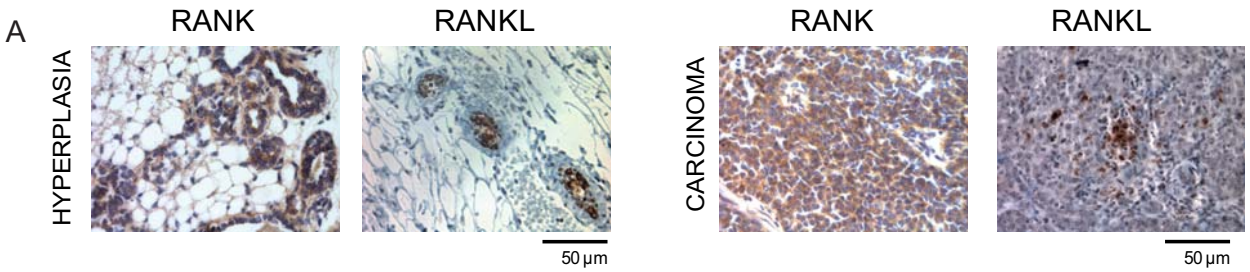
A
RANK
RANKL
RANK
RANKL
HYPERPLASIA
CARCINOMA
50 µm
50 µm

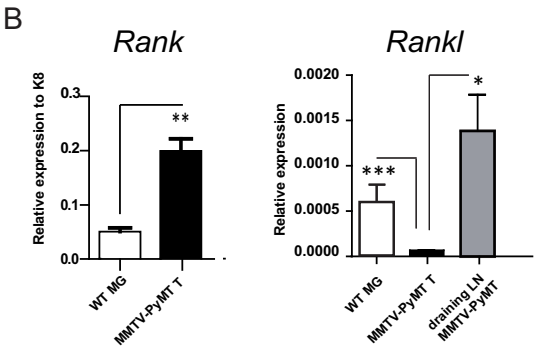
B
Rank
Rankl
Relative expression to K8
0.3
0.2
0.1
0.0
**
WT MG
MMTV-PyMT T
Relative expression
0.0020
0.0015
0.0010
0.0005
0.0000
***
*
WT MG
MMTV-PyMT T
draining LN MMTV-PyMT

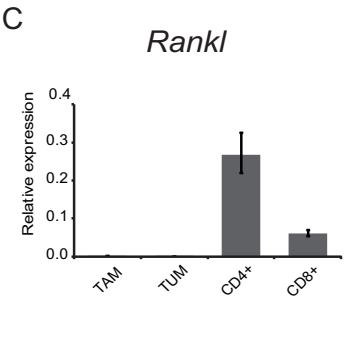
C
Rankl
Relative expression
0.4
0.3
0.2
0.1
0.0
TAM
TUM
CD4+
CD8+

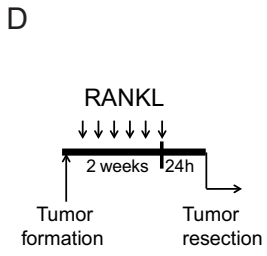
D
RANKL
2 weeks
24h
Tumor formation
Tumor resection

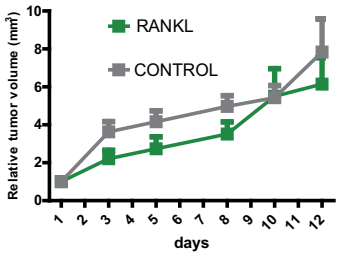
E
RANKL
CONTROL
Relative tumor volume (mm³)
10
8
6
4
2
0
1
2
3
4
5
6
7
8
9
10
11
12
days


F
secretory areas
% of total area
10
5
0
*
CONTROL
RANKL

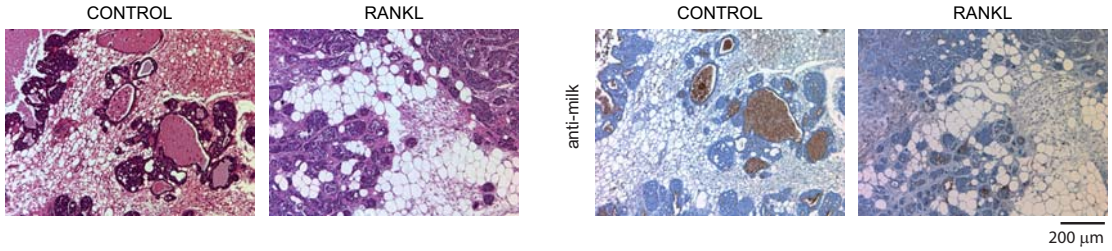
G
CONTROL
RANKL
CONTROL
RANKL
anti-milk
200 µm

Figure 2

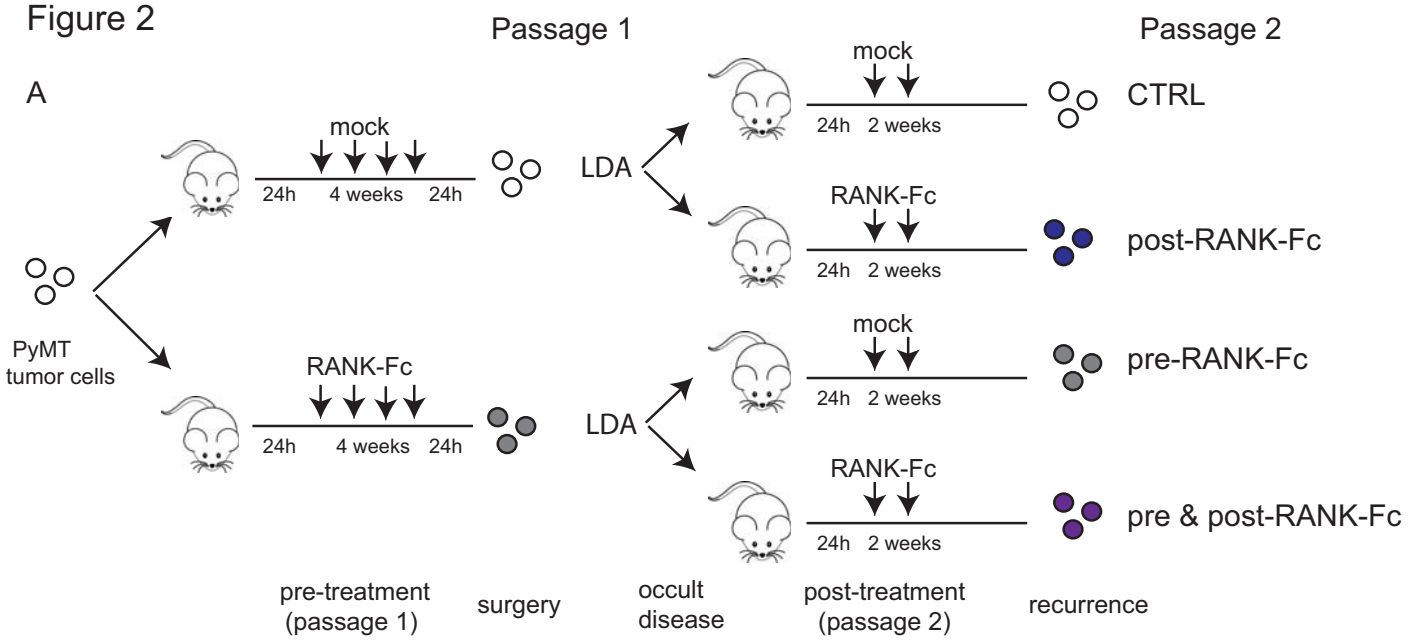

B

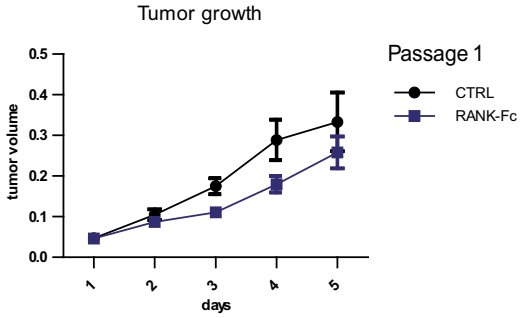

C

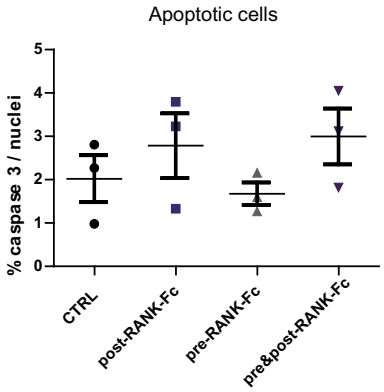

D

GROUP	N cells	N fat pad	N tumors	TIC frequency
CTRL	100,000	4	4	1/ 206 (C.I. 599 - 70.9)
	10,000	6	6	
	1,000	6	5	
	100	6	6	
post RANK-Fc	100,000	6	6	1/ 466 (C.I. 1,138-190.7)
	10,000	6	6	
	1,000	6	4	
	100	6	4	
pre RANK-Fc	100,000	6	6	1/ 1,929 (C.I. 5,431-685.1)
	10,000	6	5	
	1,000	6	5	
	100	6	2	
pre&post RANK-Fc	100,000	6	6	1/ 2,353 (C.I. 6,378 -868.3)
	10,000	6	5	
	1,000	6	3	
	100	6	3	

GROUP	P value	χ^2
CTRL vs post RANK-Fc	0.13	2.27
CTRL vs pre RANK-Fc	2.99 E-5	17.4
CTRL vs pre&post RANK-Fc	7.48 E-6	7.41
pre RANK-Fc vs pre&post RANK-Fc	0.701	0.147

E

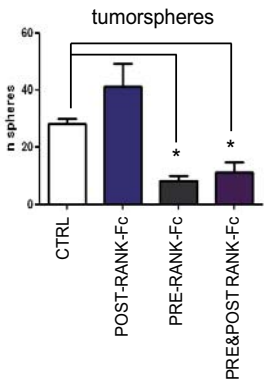

Figure 3

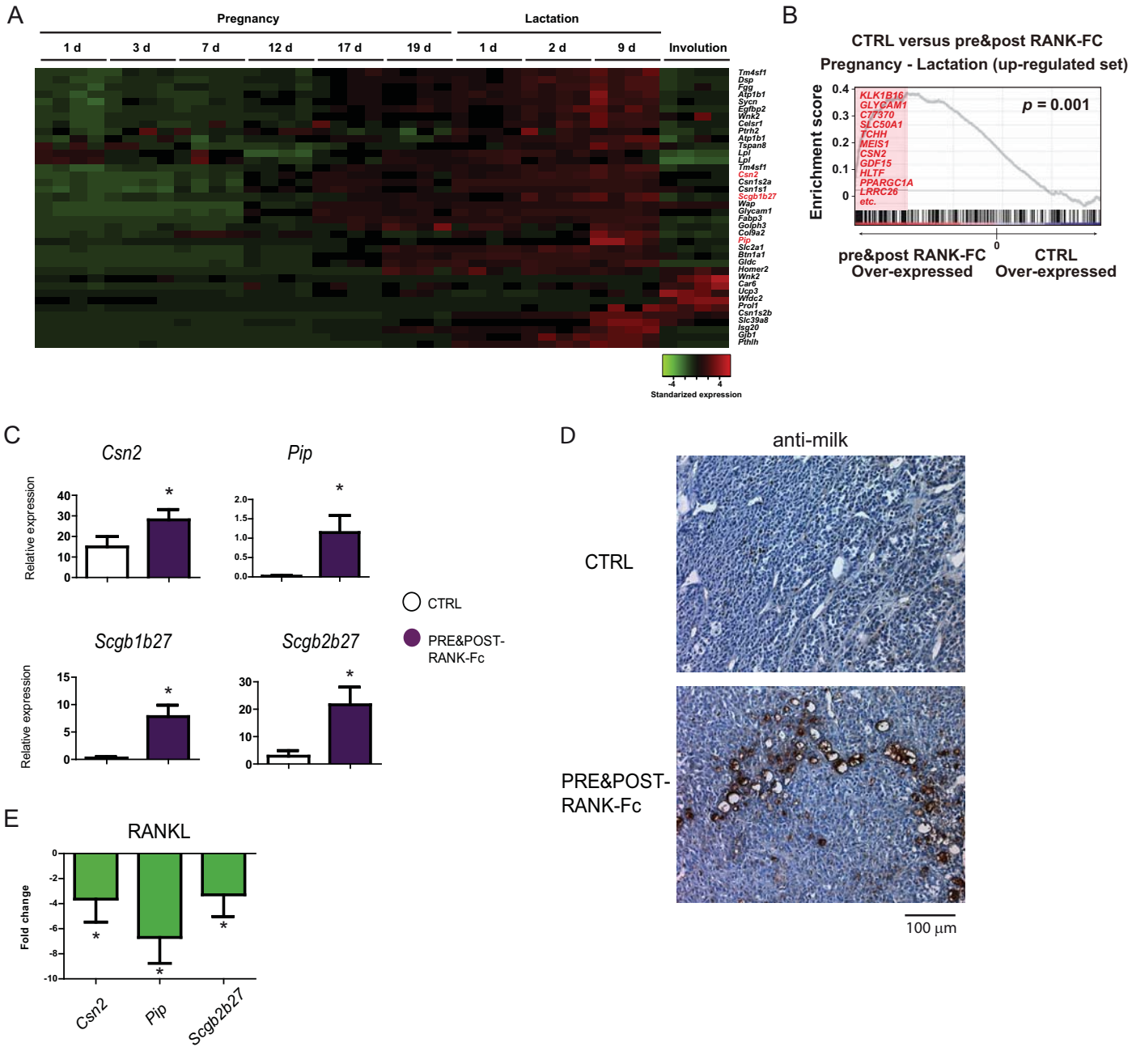
A
Pregnancy
Lactation
1 d
3 d
7 d
12 d
17 d
19 d
1 d
2 d
9 d
Involution
Tm4sf1
Dsp
Fgg
Atp1b1
Sycn
Egfbp2
Wnk2
Celsr1
Ptrh2
Atp1b1
Tspan8
Lpl
Lpl
Tm4sf1
Csn2
Csn1s2a
Csn1s1
Scgb1b27
Wap
Glycam1
Fabp3
Golph3
Col9a2
Pip
Slc2a1
Btn1a1
Gldc
Homer2
Wnk2
Car6
Ucp3
Wfdc2
Prol1
Csn1s2b
Slc39a8
Isg20
Gjb1
Pthlh
-4
4
Standarized expression
B
CTRL versus pre&post RANK-FC
Pregnancy - Lactation (up-regulated set)
Enrichment score
0.4
0.3
0.2
0.1
0
p = 0.001
KLK1B16
GLYCAM1
C77370
SLC50A1
TCHH
MEIS1
CSN2
GDF15
HLTF
PPARGC1A
LRRC26
etc.
0
pre&post RANK-FC
Over-expressed
CTRL
Over-expressed
C
Csn2
Pip
Relative expression
40
30
20
10
0
2.0
1.5
1.0
0.5
0.0
CTRL
PRE&POST-
RANK-Fc
Scgb1b27
Scgb2b27
15
10
5
0
30
20
10
0
D
anti-milk
CTRL
PRE&POST-
RANK-Fc
100 µm
E
RANKL
Fold change
0
-2
-4
-6
-8
-10
Csn2
Pip
Scgb2b27

Figure 4

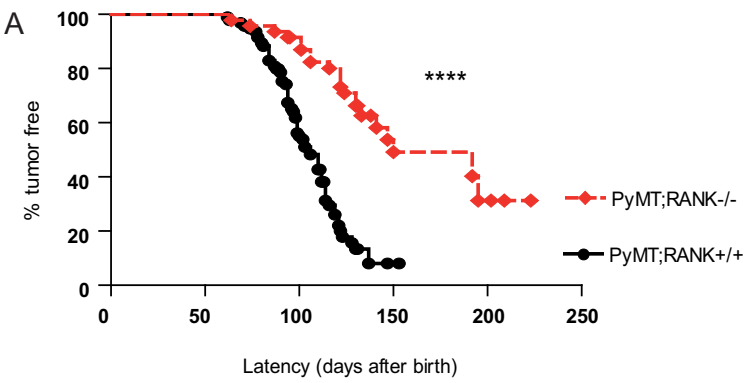
A
% tumor free
100
80
60
40
20
0
0
50
100
150
200
250
Latency (days after birth)
****
PyMT;RANK-/-
PyMT;RANK+/+

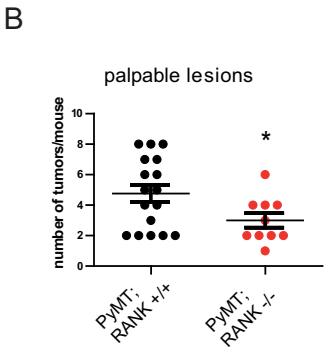
B
palpable lesions
number of tumors/mouse
10
8
6
4
2
0
*
PyMT; RANK +/+
PyMT; RANK -/-

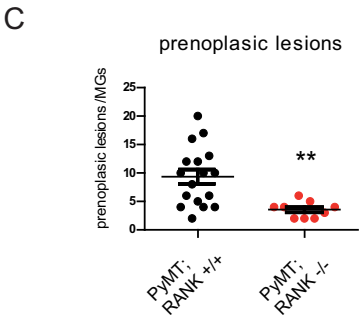
C
prenoplasic lesions
prenoplasic lesions /MGs
25
20
15
10
5
0
**
PyMT; RANK +/+
PyMT; RANK -/-

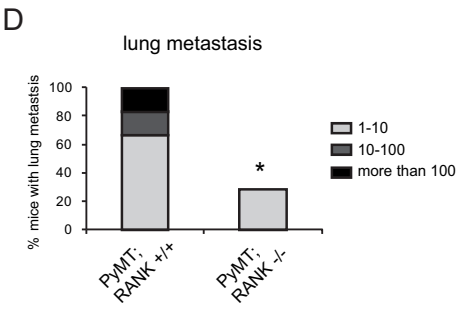
D
lung metastasis
% mice with lung metastsis
100
80
60
40
20
0
*
1-10
10-100
more than 100
PyMT; RANK +/+
PyMT; RANK -/-

Figure 5

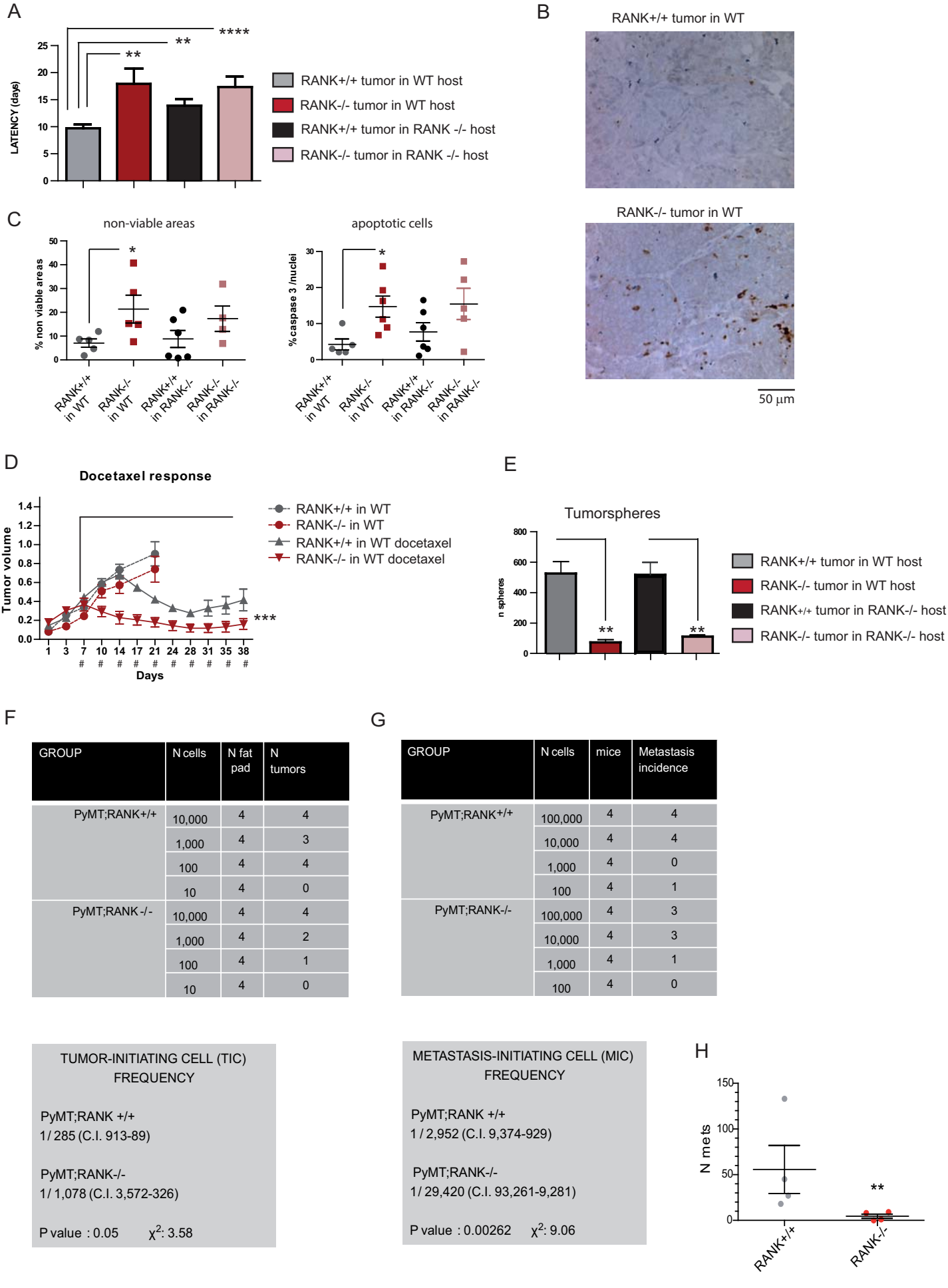

F

GROUP	N cells	N fat pad	N tumors
PyMT;RANK+/+	10,000	4	4
	1,000	4	3
	100	4	4
	10	4	0
PyMT;RANK -/-	10,000	4	4
	1,000	4	2
	100	4	1
	10	4	0

G

GROUP	N cells	mice	Metastasis incidence
PyMT;RANK+/+	100,000	4	4
	10,000	4	4
	1,000	4	0
	100	4	1
PyMT;RANK-/-	100,000	4	3
	10,000	4	3
	1,000	4	1
	100	4	0

TUMOR-INITIATING CELL (TIC) FREQUENCY

PyMT;RANK +/+
1/ 285 (C.I. 913-89)

PyMT;RANK-/-
1/ 1,078 (C.I. 3,572-326)

P value : 0.05 χ^2: 3.58

METASTASIS-INITIATING CELL (MIC) FREQUENCY

PyMT;RANK +/+
1 / 2,952 (C.I. 9,374-929)

PyMT;RANK-/-
1/ 29,420 (C.I. 93,261-9,281)

P value : 0.00262 χ^2: 9.06

H

Figure 6

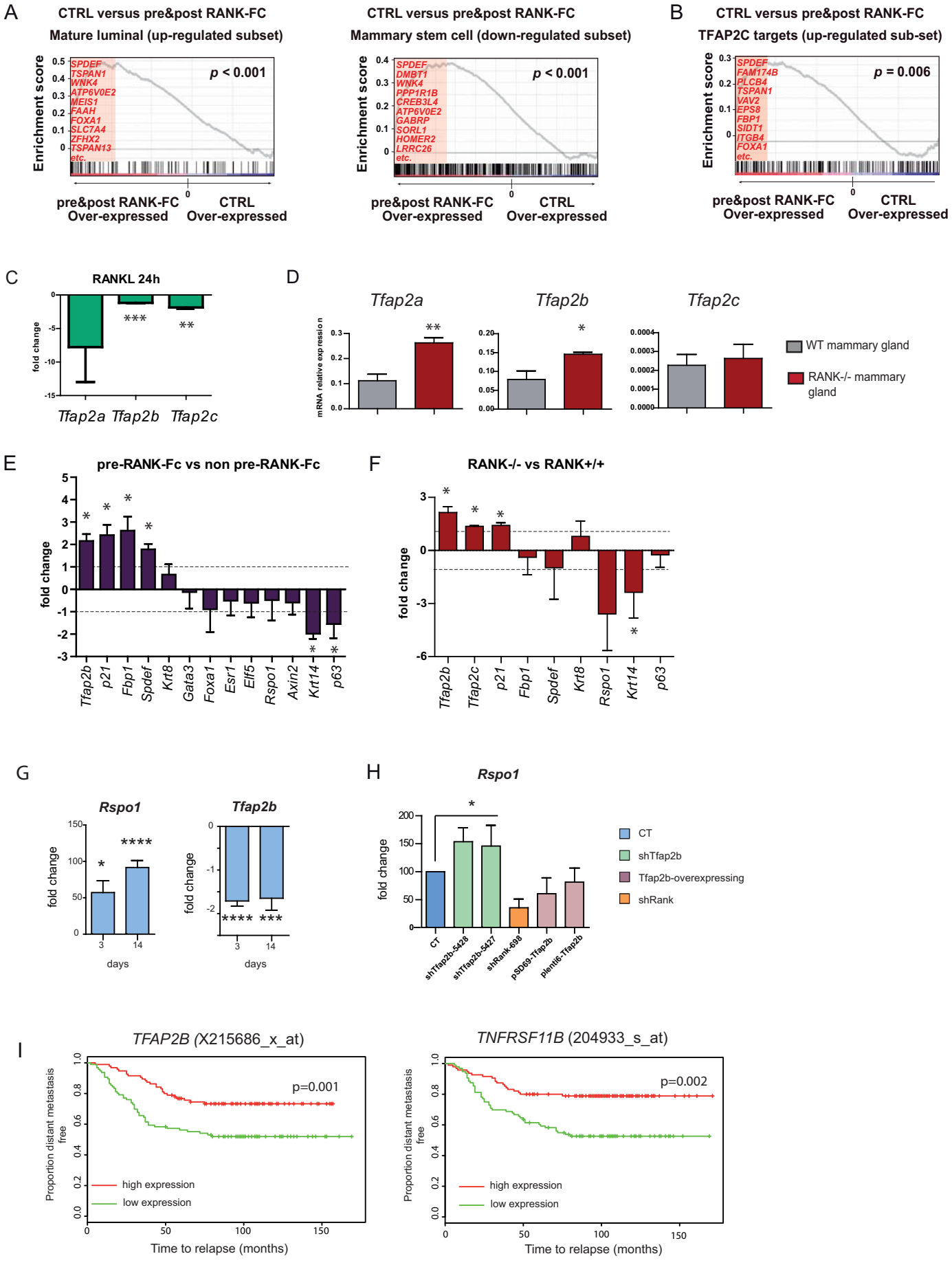
A
CTRL versus pre&post RANK-FC
Mature luminal (up-regulated subset)
Enrichment score
SPDEF
TSPAN1
WNK4
ATP6V0E2
MEIS1
FAAH
FOXA1
SLC7A4
ZFHX2
TSPAN13
etc.
p < 0.001
pre&post RANK-FC Over-expressed
CTRL Over-expressed
CTRL versus pre&post RANK-FC
Mammary stem cell (down-regulated subset)
SPDEF
DMBT1
WNK4
PPP1R1B
CREB3L4
ATP6V0E2
GABRP
SORL1
HOMER2
LRRC26
etc.
p < 0.001
pre&post RANK-FC Over-expressed
CTRL Over-expressed
B
CTRL versus pre&post RANK-FC
TFAP2C targets (up-regulated sub-set)
SPDEF
FAM174B
PLCB4
TSPAN1
VAV2
EPS8
FBP1
SIDT1
ITGB4
FOXA1
etc.
p = 0.006
pre&post RANK-FC Over-expressed
CTRL Over-expressed
C
RANKL 24h
fold change
***
**
Tfap2a Tfap2b Tfap2c
D
Tfap2a
Tfap2b
Tfap2c
mRNA relative expression
WT mammary gland
RANK-/- mammary gland
E
pre-RANK-Fc vs non pre-RANK-Fc
fold change
Tfap2b p21 Fbp1 Spdef Krt8 Gata3 Foxa1 Esr1 Elf5 Rspo1 Axin2 Krt14 p63
F
RANK-/- vs RANK+/+
fold change
Tfap2b Tfap2c p21 Fbp1 Spdef Krt8 Rspo1 Krt14 p63
G
Rspo1
Tfap2b
fold change
days
H
Rspo1
fold change
CT
shTfap2b
Tfap2b-overexpressing
shRank
CT
shTfap2b-5428
shTfap2b-5427
shRank-698
pSD69-Tfap2b
plenti6-Tfap2b
I
TFAP2B (X215686_x_at)
p=0.001
Proportion distant metastasis free
high expression
low expression
Time to relapse (months)
TNFRSF11B (204933_s_at)
p=0.002
Proportion distant metastasis free
high expression
low expression
Time to relapse (months)

Figure 7

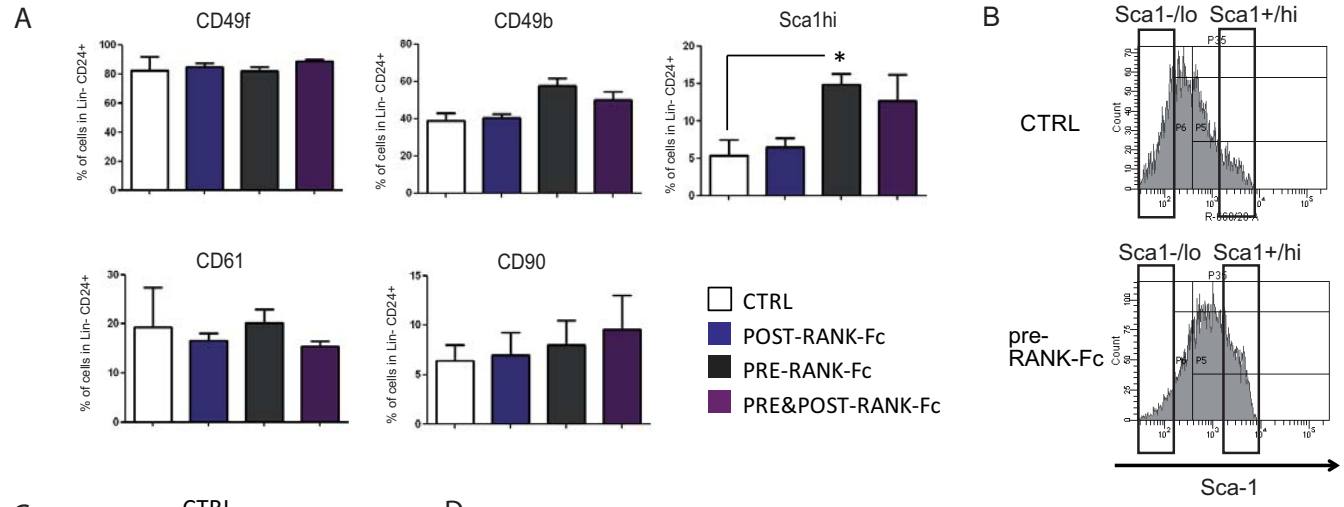

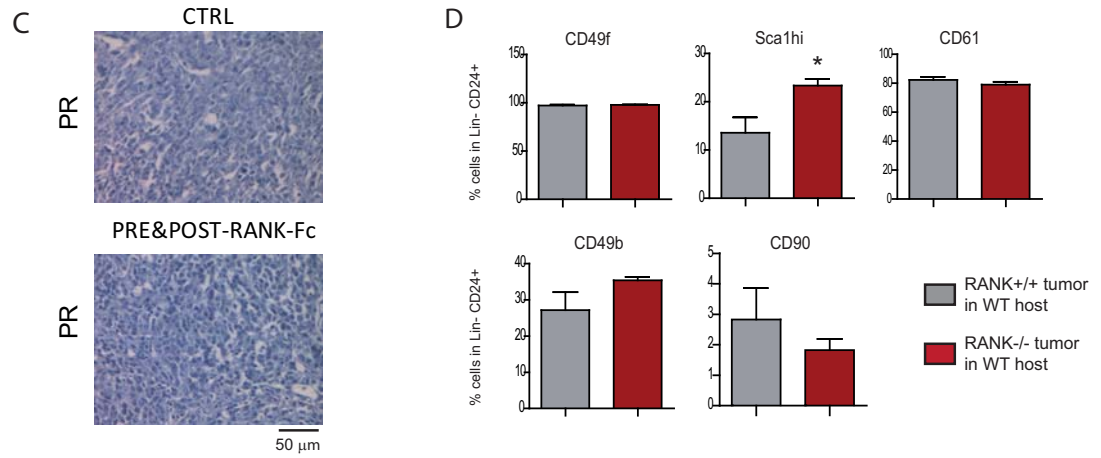

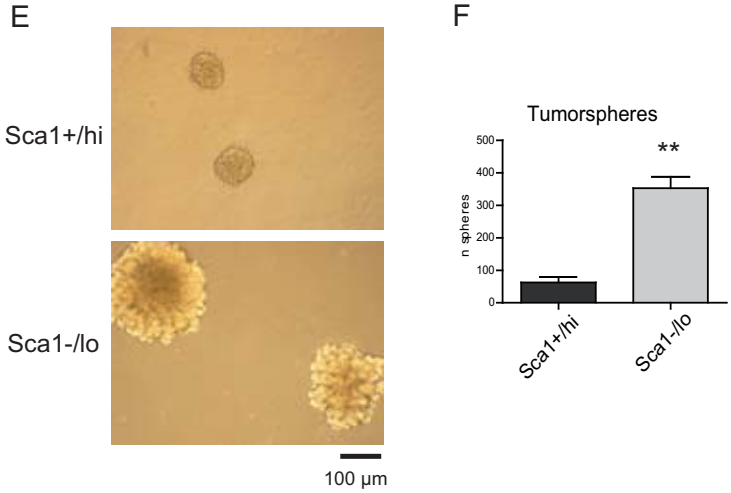

G

GROUP	N cells	N fat pad	N tumors
Sca1+/hi	100,000	4	3
	10,000	4	3
	1,000	4	2
	100	4	3
Sca1-/lo	100,000	4	4
	10,000	4	4
	1,000	4	4
	100	4	3

TICs TUMOR INITIATING CELL FREQUENCY (ELDA)

Sca1+/hi : 1/ 15767.4 (C.I. 56295 - 4416.4)

Sca1-/lo : 1/ 72.6 (C.I. 246 - 21.7)

P value: 1.04E-11 $\chi^2 = 46.3$